Quarterly Reviews of Biophysics **36**, 1 (2003), pp. 71–89. © 2003 Cambridge University Press
DOI: 10.1017/S0033583502003839 Printed in the United Kingdom

Photosystem II: the engine of life

James Barber

Imperial College of Science, Technology & Medicine, Wolfson Laboratories, Department of Biological Sciences, London SW7 2AY, UK

Abstract. Photosystem II (PS II) is a multisubunit membrane protein complex, which uses light energy to oxidize water and reduce plastoquinone. High-resolution electron cryomicroscopy and X-ray crystallography are revealing the structure of this important molecular machine. Both approaches have contributed to our understanding of the organization of the transmembrane helices of higher plant and cyanobacterial PS II and both indicate that PS II normally functions as a dimer. However the high-resolution electron density maps derived from X-ray crystallography currently at 3·7/3·8 Å, have allowed assignments to be made to the redox active cofactors involved in the light-driven water–plastoquinone oxidoreductase activity and to the chlorophyll molecules that absorb and transfer energy to the reaction centre. In particular the X-ray work has identified density that can accommodate the four manganese atoms which catalyse the water-oxidation process. The Mn cluster is located at the lumenal surface of the D1 protein and approximately 7 Å from the redox active tyrosine residue (Y_Z) which acts an electron/proton transfer link to the primary oxidant $P680^{\bullet+}$. The lower resolution electron microscopy studies, however, are providing structural models of larger PS II supercomplexes that are ideal frameworks in which to incorporate the X-ray derived structures.

1. Introduction

Photosystem II (PS II) is a multisubunit complex embedded in the thylakoid membranes of plants, algae and cyanobacteria (see Fig. 1). This photosynthetic enzyme catalyses the most

Tel.: 44 2075945266; Fax: 44 2075945267; E-mail: j.barber@ic.ac.uk

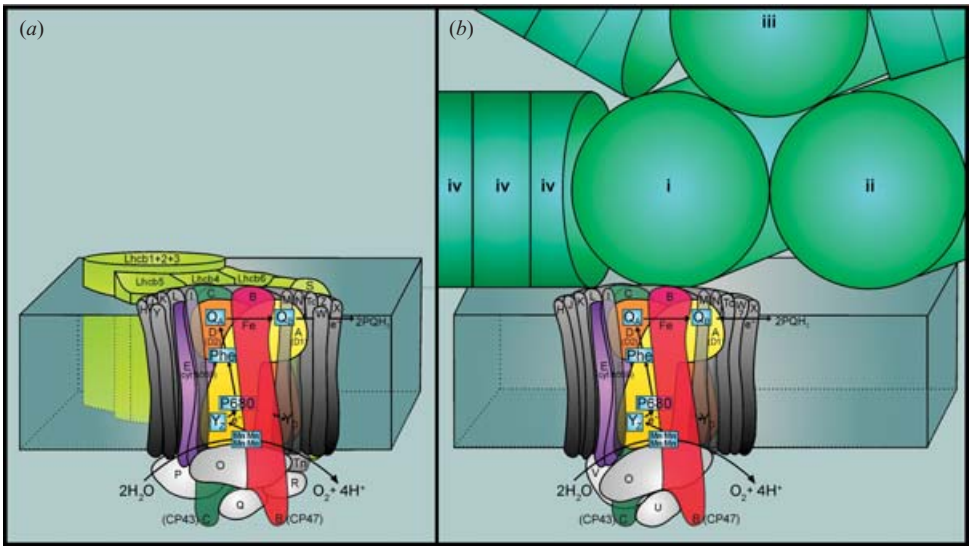

Fig. 1. Illustration of the structure and subunit composition of PS II. (*a*) Higher plants and green algae. (*b*) Phycobilisome-containing cyanobacteria. The intrinsic and extrinsic proteins are labelled according to the gene nomenclature (e.g. *psb*A = A; see Table 1) with common designations given for the major subunits (e.g. A = D1 protein). The outer light-harvesting proteins are coloured light green for the plant systems (intrinsic Lhcb/Cab proteins) and blue-green for the cyanobacterial systems (extrinsic phycobiliproteins forming a phycobilisome where i, ii and iii are allophycocyanin rods depicted at the appropriate size compared with the width of the PS II core monomer) and iv are discs of other phycobiliproteins which make up the rods of the phycobilisome (e.g. C-phycocyanin). The electron transfer pathway from water oxidation to plastoquinone reduction (PQH_2) is shown (see text).

thermodynamically demanding reaction in biology: namely the splitting of water into dioxygen and reducing equivalents. The reaction is driven by solar energy and underpins the survival of essentially all life on our planet. It supplies the oxygen we breath, it maintains the ozone layer needed to protect us from UV radiation and, of course, it supplies the reducing equivalents necessary to fix carbon dioxide to organic molecules which creates biomass, food and fuel. For these reasons it is truly the 'engine of life' and its appearance approximately 2 billion years ago represented the 'big bang' of evolution. An essential prerequisite for understanding and possibly mimicking the molecular mechanisms of PS II is a detailed understanding of the three-dimensional (3D) structure of the participating macromolecular subunits, including those directly involved in the water-splitting reaction. Indeed unravelling the mechanism of this reaction within a structural framework is today one of the greatest challenges in photosynthesis research and biology in general. Here I review how high-resolution electron microscopy and X-ray crystallography are contributing to the goal of obtaining a full description of the molecular processes by which PS II functions as a light-driven water oxidase.

2. Electron transfer in PS II

Prior to recent structural work, a range of biochemical and biophysical techniques had provided a good understanding of the events which give rise to the primary and secondary electron transfer processes leading to water oxidation (reviewed by Diner & Babcock, 1996). These processes are initiated by the absorption of light energy by the many chlorophyll and other

https://doi.org/10.1017/S0033583502003839 Published online by Cambridge University Press

pigment molecules associated with PS II. The nature of these PS II light-harvesting antenna systems vary under different growth conditions and with different types of organisms. However, within the PS II core complex only chlorophyll *a* (chl *a*) and β-carotene are found,[1] bound mainly to the CP47 and CP43 proteins (B and C subunits respectively and coloured red and green in Fig. 1). In total there are approximately 35 chl *a* and approximately 10 β-carotene per PS II core. The excitation energy absorbed by these pigments is then transferred to the reaction centre (RC) composed of the D1 and D2 proteins (A and D subunits respectively, coloured yellow and orange in Fig. 1). Together these RC proteins bind all the redox active cofactors involved in the energy conversion process and the following sequence of reactions occurs. A special form of chl *a*, P680 acts as an exciton trap and is converted to a strong reducing agent after excitation (P680*). P680* reduces a pheophytin molecule (Phe) within a few picoseconds to form the radical pair state $P680^{\bullet+}Phe^{\bullet-}$. Within a few hundred picoseconds, $Phe^{\bullet-}$ reduces a plastoquinone molecule bound to the D2 protein (Q_A) to produce $P680^{\bullet+}PheQ_A^{-}$. $P680^{\bullet+}$, which has a very high redox potential (>1 V), oxidizes a tyrosine residue (Y_Z) of the D1 protein (Tyr161) to form $Y_Z^{\bullet+}P680PheQ_A^{-}$ on a nanosecond timescale. Note that another tyrosine (Y_D), located in a similar position on the D2 protein, is also oxidized by $P680^{\bullet+}$ but this is a single event occurring on the first photochemical turnover after an extended dark period. It is generally believed that $Y_Z^{\bullet+}$ on the active electron transfer branch of water oxidation is deprotonated to form a neutral radical $Y_Z^{\bullet}$. In the millisecond time domain Q_A^{-} reduces a second plastoquinone associated with the D1 protein (Q_B) to form $Y^{\bullet}PheQ_AQ_B^{-}$. At about the same time the neutral tyrosine radical ($Y_Z^{\bullet}$) extracts an electron, and probably a proton, from a cluster of four manganese atoms that bind the two substrate water molecules. A second photochemical turnover reduces Q_B^{-} to Q_B^{2-} which is then protonated to plastoquinol and released from the D1 protein into the lipid bilayer to be subsequently oxidized by photosystem I (PS I) via the cytochrome b_6f complex. Two further photochemical turnovers provide the manganese cluster with a total of four oxidizing equivalents, which are used to oxidize two water molecules to dioxygen. Each oxidation state is represented in an S-state cycle shown and explained in Fig. 2. In addition to these reactions, side reactions can occur under some conditions including the oxidation of a high potential cytochrome bound within the PS II core complex [cytochrome *b*559 (cyt *b*559)], a β-carotene molecule and a chl *a* molecule (Chl_Z) (Telfer *et al.* 1991; Hanley *et al.* 1999; Tracewell *et al.* 2001). These side reactions occur on the millisecond timescale and therefore do not compete with the main electron transfer pathway leading to water oxidation. Indeed, they probably only occur when water oxidation becomes limited and thus provide a protective mechanism against the detrimental reactions resulting from the very high redox potential of the long-lived P680 radical cation (Barber & De Las Rivas, 1993; Barber, 1994; Stewart & Brudvig, 1998).

3. $(Mn)_4$ cluster and mechanism of water oxidation

The electron transfer reactions that occur on the reducing side of PS II and bring about the reduction of plastoquinone to plastoquinol are remarkably similar to those that occur in the RCs of purple photosynthetic bacteria (Michel & Deisenhofer, 1988). It is, however, the oxidizing

[1] Recently it has been discovered that an oxyphotobacterium *Acaryochloris marina* contains almost entirely chl *d* (Miyashita *et al.* 1996) which is bound to PS II and PS I core proteins. Moreover, the primary donor of PS I is also composed of chl *d* (Hu *et al.* 1998). Although likely, it has yet to be proven that the low level of chl *a* present in this organism functions as the primary donor of PS II.

https://doi.org/10.1017/S0033583502003839 Published online by Cambridge University Press

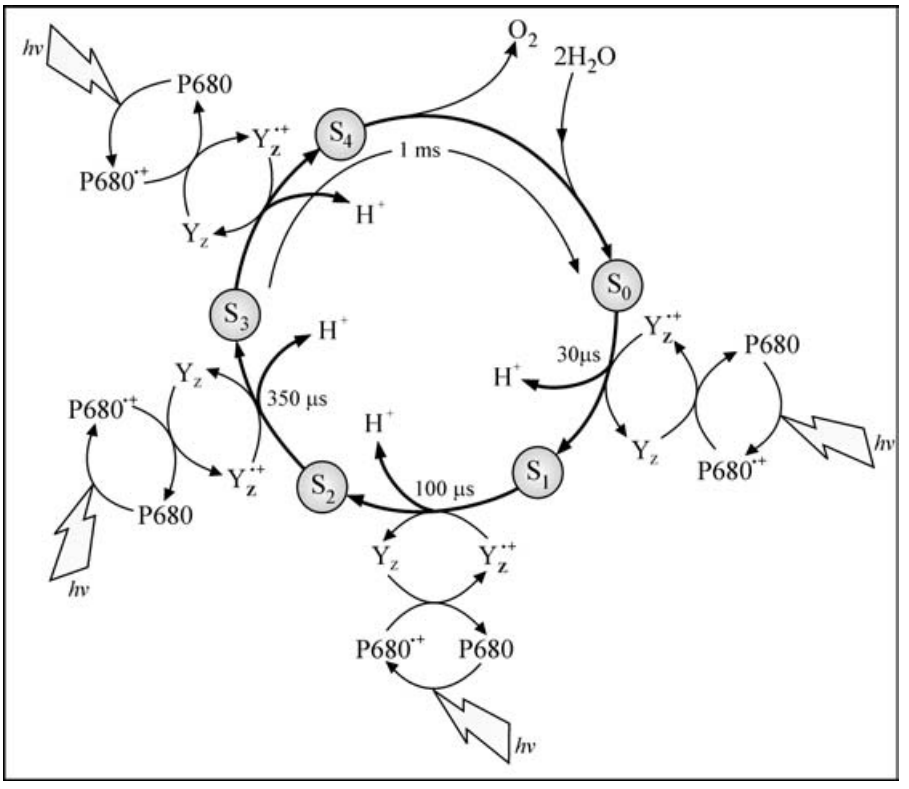

Fig. 2. The S-state cycle for the oxygen evolution reaction as first suggested by Kok *et al.* (1970) modified to accommodate the model proposed by Babcock and colleagues (Hoganson & Babcock, 1997; Tommos & Babcock, 2000) which advocated that each photoinduced step of the S-state cycle (S_0–S_4) involves the concerted removal of an electron and a proton from two bound water molecules. Other proposed mechanisms do not invoke a hydrogen abstraction on each step of the cycle but do support the general concept that the two water substrate molecules are bound at the S_0 state and undergo oxidation throughout the S-state cycle (Hanmann & Junge, 1999; Vrettos *et al.* 2001).

side that makes PS II so unique. The high redox potential of $P680^{\bullet+}$ is required to oxidize water and the four oxidizing equivalents generated by the four photochemical turnovers of the S-state cycle (see Fig. 2) are localized on or near the $(Mn)_4$ cluster. There is increasing evidence to suggest that these four oxidizing equivalents do not accumulate but are utilized throughout the S-state cycle to extract electrons and protons from two substrate water molecules bound to the $(Mn)_4$ cluster at the S_0 state. Moreover, it has been known for some time that calcium and chloride ions are required for water-oxidation catalysis and are believed to be located close to the $(Mn)_4$ cluster (Debus, 1992). One possible mechanism for the subsequent oxidation processes involves the concerted removal of a proton and electron from the two substrate water molecules at each step of the S-state cycle. This hydrogen abstraction model was proposed by Babcock and co-workers (Hoganson & Babcock, 1997; Tommos & Babcock, 2000) and is shown in Fig. 3*a*. In this scheme the deprotonation of $Y_Z^{\bullet+}$ to create a neutral radical $Y_Z^{\bullet}$ facilitates its subsequent reduction by accepting an electron and proton on each step of the S-state cycle. The radical states formed on the substrate water intermediates are stabilized by increases in oxidation level of the $(Mn)_4$ cluster. As a proton, as well as an electron, is ejected at each step of the S-state cycle the increase in oxidation of the $(Mn)_4$ cluster does not

https://doi.org/10.1017/S0033583502003839 Published online by Cambridge University Press

impose any coulombic restrictions because the system remains electroneutral. However, there is experimental evidence to suggest that this electroneutral scheme does not happen and that the S_1–S_2 transition involves only electron transfer from the $(Mn)_4$ cluster. With this in mind alternative schemes to describe water oxidation have been suggested. For example, Brudvig and colleagues (Vrettos *et al.* 2001) have proposed the scheme shown in Fig. 3*b*. Again it is believed that the two substrate water molecules are bound at the S_0 state with one associated with Ca^{2+}. Their mechanism requires that during the S-state cycle one of the Mn becomes highly oxidized to Mn(V) and a Ca^{2+} acts as a Lewis acid by facilitating a nucleophilic attack on an electron-deficient Mn(V)═O intermediate in order to allow the O—O bond to form. Hydrogen atom abstraction is proposed for all steps except for the S_1–S_2 transition.

The two schemes shown in Fig. 3 are reliant on $Y_Z^{\bullet}$ (i.e. $Y_ZO^{\bullet}$) to act as a H^+ as well as an electron acceptor. In the absence of a high-resolution structural model it has been proposed that D1–His190 is hydrogen bonded to Y_Z and that the phenolic proton of tyrosine is transferred to this histidine. In turn this histidine transfers each proton generated by the water-oxidation process to a second acceptor and a domino deprotonation occurs, eventually giving rise to proton release into the lumen. Here again, the measured proton release pattern does not seem to agree with Babcock's electroneutral theory for water oxidation and has been measured to be 1, 0, 1, 2 for S_0–S_4 by Junge and colleagues (Hanmann & Junge, 1999). However, because the catalytic site for water oxidation is buried within the large protein mass attached to the lumenal membrane surface, it is difficult to be sure if this stoichiometry is a true reflection of the proton release pattern from the two substrate water molecules.

In order to obtain a more reliable chemical mechanism for water oxidation, structural information is required at better resolution than is currently available. Ideally structures need to be obtained for each S state of the S_0–S_4 cycle and at a resolution better than 2.5 Å. Nevertheless, as described below, high-resolution electron microscopy and X-ray crystallography have paved the way towards this goal.

4. Organization and structure of the protein subunits

The RC core complex contains at least 15 transmembrane proteins and three well-characterized extrinsic proteins (see Table 1). The main intrinsic proteins are the CP47 and CP43 chlorophyll-binding proteins and the intimately associated D1 and D2 RC proteins. Also closely positioned to the D1/D2 proteins is cyt *b*559 which is composed of two subunits PsbE and PsbF (α- and β-subunits respectively and coloured magenta in Fig. 1). In addition there are 10 or more single transmembrane helical low-molecular-weight subunits (see Table 1). None of these small subunits (coloured grey in Fig. 1) have redox active centres and their functions are unknown. Taken together these intrinsic membrane proteins making up the PS II core complex give rise to at least 34 transmembrane helices. The newly characterized PsbZ protein (Cinque *et al.* 2001) could also be present and is predicted to have a single transmembrane helix. The extrinsic proteins are the 33 kDa PsbO, 23 kDa PsbP and 16 kDa PsbQ in higher plants and green algae but in the case of red algae and cyanobacteria the extrinsic proteins are the 33 kDa PsbO, 10·5 kDa PsbU and 15 kDa PsbV where the latter is a cytochrome (cyt *c*550). The products of the *psb*R gene (Ljungberg *et al.* 1986) and *psb*T_n gene (Kapazoglou *et al.* 1995) (see Fig. 1*a* and Table 1) may also be additional lumenally bound, extrinsic proteins in higher plants. These extrinsic proteins are located close to the $(Mn)_4$ cluster on the donor side of PS II and seem to stabilize and protect the water-oxidation site and provide an environment for

https://doi.org/10.1017/S0033583502003839 Published online by Cambridge University Press

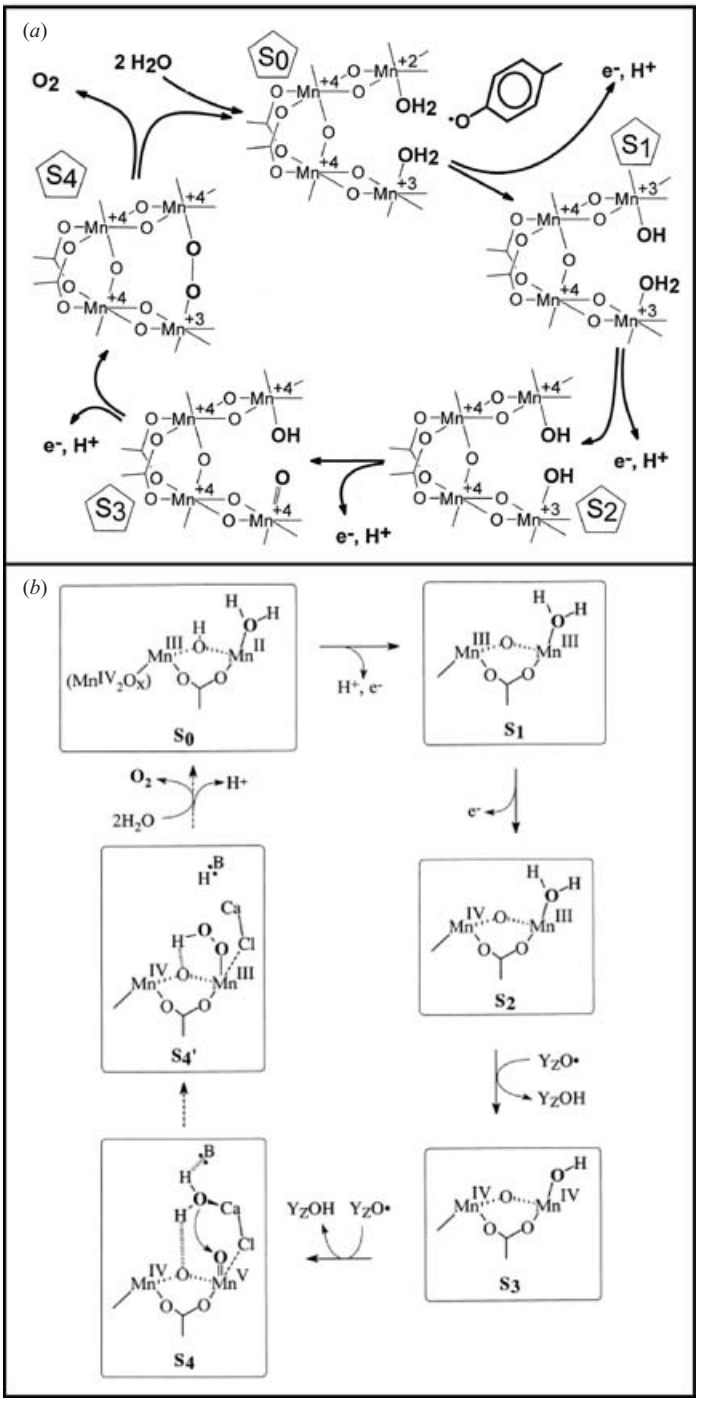

Fig. 3. Examples of two mechanistic reaction schemes proposed for H_2O oxidation. (*a*) The 'hydrogen' abstraction scheme of Babcock and colleagues taken from Hoganson & Babcock (1997). (*b*) The 'high valency' mechanism of Brudvig and colleagues taken from Vrettos *et al.* (2001). Although the Babcock scheme assumed a 'dimer of dimer' model for the $(Mn)_4$ cluster it is not dependent on this particular configuration and can be accommodated, according to the recent X-ray data of Zouni *et al.* (2001). The recent X-ray data also does not negate the Brudvig model but note that in this scheme only two Mn atoms

https://doi.org/10.1017/S0033583502003839 Published online by Cambridge University Press

Table 1. *Protein subunits of PS II core reaction centre complex*

Gene	Subunit	Mass (kDa)	No. of transmembrane α-helices
*psb*A (c)	D1	38·021 (S)	5
*psb*B (c)	CP47	56·278 (S)	6
*psb*C (c)	CP43	50·066 (S)	6
*psb*D (c)	D2	39·418 (S)	5
*psb*E (c)	α-cyt *b*559	9·255 (S)	1
*psb*F (c)	β-cyt *b*559	4·409 (S)	1
*psb*H (c)	H protein	7·697 (S)	1
*psb*I (c)	I protein	4·195 (S)	1
*psb*J (c)	J protein	4·116 (P)	1
*psb*K (c)	K protein	4·283 (S)	1
*psb*L (c)	L protein	4·366 (S)	1
*psb*M (c)	M protein	3·755 (P)	1
*psb*N (c)	N protein	4·722 (T)	1
*psb*O (n)	33 kDa O protein	26·539 (S)	0
*psb*P (n)	23 kDa P protein	20·210 (S)	0
*psb*Q (n)	16 kDa Q protein	16·523 (S)	0
*psb*R (n)	R protein	10·236 (S)	0
*psb*Tc (c)	T_C protein	3·849 (S)	1
psbT_n (n)	T_n protein	3·171 (A)	0
*psb*U	U protein	10·491 (Sy)	0
*psb*V	V protein	15·121 (Sy)	0
*psb*W (n)	W protein	5·928 (S)	1
*psb*X (n)	X protein	4·225 (S)	1

These proteins are products of the *psb*A to *psb*X genes that occur in all types of oxygenic organisms except possibly PsbW. In eukaryotic organisms the *psb* genes are located in either the chloroplast (c) or nuclear (n) genes. The molecular masses of the mature PsbA–PsbX proteins are calculated from the protein sequences reported in the SwissProt database using the MacBioSpec program (Sciex Corp., Thornhill, ON, Canada) for spinach (S), pea (P), tobacco (T), *Arabidopsis* (A) and *Synechocystis* PCC6803 (Sy). The core complex may contain the product of the *psb*Z gene (Cinque *et al.* 2001).

optimizing the Ca^{2+} and Cl^- levels, required as cofactors for the water-splitting reaction. Why red algae and cyanobacteria have a cytochrome on their lumenal surfaces is a mystery since this cytochrome has a very low potential and has no photo-induced redox activity.

Sequence analyses and hydropathy plots suggested that the D1 and D2 proteins of PS II RC were structurally similar to the L and M subunits of the purple bacterial RC (Barber, 1987; Michel & Deisenhofer, 1988) for which an X-ray structure was determined more than 15 years ago (Deisenhofer *et al.* 1985) and led to the award of the Nobel Prize for Chemistry in 1988. This work was confirmed in 1998 when a 3D structure of a subcomplex of PS II isolated from spinach was obtained by electron crystallography at a resolution of 8 Å (Rhee *et al.* 1997, 1998). Both D1 and D2 subunits consist of five transmembrane helices related by a pseudo-twofold axis (shown in Fig. 4*a* as yellow and orange cylinders for D1 and D2 proteins respectively). Using electron crystallography it was also possible to assign six transmembrane helices to CP47, showing for the first time that these helices were arranged in a circular manner as three pairs (shown in Fig. 4*a* as red cylinders). It was noted that this arrangement was similar to the six N-terminal transmembrane helices of the PS I RC proteins that had been revealed by X-ray

are involved in the water oxidation chemistry. For clarity the two Mn atoms which do not undergo redox changes during S-state advancement [assumed to be $Mn(IV)_2O_x$] are omitted beyond S_0.

https://doi.org/10.1017/S0033583502003839 Published online by Cambridge University Press

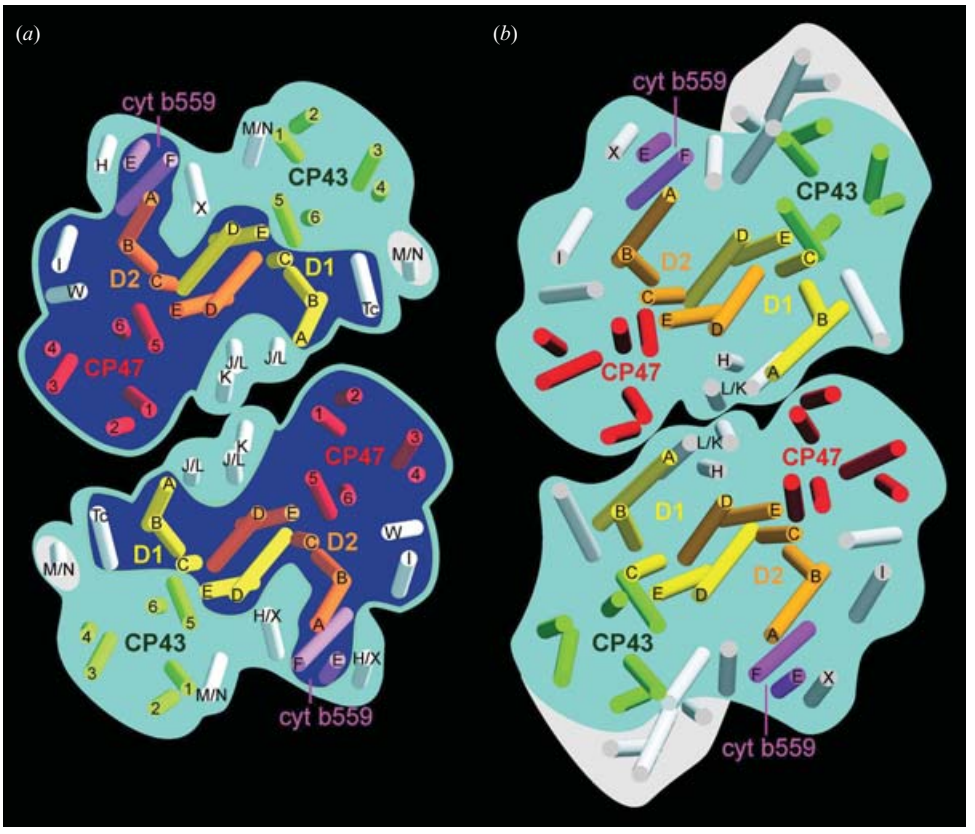

Fig. 4. Comparison of the transmembrane helix organization of PS II core dimer of (*a*) higher plants (spinach) and (*b*) cyanobacteria (*Synechococcus elongatus*) derived from electron (Hankamer *et al.* 2001a, b) and X-ray (Zouni *et al.* 2001) crystallography respectively. The transmembrane helices of D1 (yellow), D2 (orange), CP47 (red), CP43 (green) and cyt *b*559 seem to be in identical positions. This is also true for 9 of the single transmembrane low-molecular-weight subunits shown in light grey. However, the white background highlights differences between the two structural models: *S. elongatus* has 3 additional helices close to CP43 while the spinach structure suggests an additional transmembrane helix on the periphery of the complex on the D1/CP43 side (designated M/N). The dark blue region in (*a*) shows the helix organization of the spinach CP47 RC subcomplex derived from Rhee *et al.* (1998) but modified by the removal of two helices adjacent to helix B of the D1 and D2 proteins which were assigned to densities which in retrospect were due to $Chl_{Z\text{-}D1}$ and $Chl_{Z\text{-}D2}$ (see Fig. 5). The assignment of the small subunits is tentative in both structures as described in Zouni *et al.* (2001) and Hankamer *et al.* (2001b). (The figure is taken from Hankamer *et al.* 2001b.)

crystallography initially at 4 Å (Krauss *et al.* 1996) but now at 2·5 Å resolution (Jordan *et al.* 2001; Saenger *et al.* 2002). This structural homology indicates that PS II and PS I have a common evolutionary origin (Rhee *et al.* 1998; Schubert *et al.* 1998). Also assigned in the 3D map of PS II, derived from high-resolution electron cryomicroscopy (cryo-EM), were seven other transmembrane helices with two of them tentatively identified as the α- and β-subunit (PsbE and PsbF proteins respectively) of cyt *b*559 (Rhee, 2001) (shown in Fig. 4*a* as magenta cylinders, labelled E and F).

This pioneering electron crystallographic approach was extended to the analyses of 2D crystals of the PS II core dimer complex isolated from spinach leading initially to the publication of a 3D structure based on negative stained crystals (Morris *et al.* 1997). This was followed up with

https://doi.org/10.1017/S0033583502003839 Published online by Cambridge University Press

cryo-EM analyses, first to yield a projection map in 1999 (Hankamer *et al.* 1999) and later a 3D structure in 2001 (Hankamer *et al.* 2001a). The cryo-EM studies provided the first direct evidence that the transmembrane helices of CP43 (shown in Fig. 4*a* as green cylinders) were arranged in the same manner as CP47 but positioned on the opposite side of the RC proteins and related to those of CP47 by the same pseudo-two-fold axis relating the D1 and D2 helices. In addition to the 22 transmembrane helices of D1/D2/CP43/CP47 proteins, each PS II monomer contained a further 10 transmembrane helices (shown as light grey cylinders in Fig. 4*a*) excluding the two tentatively assigned to cyt *b*559. It was also concluded that two transmembrane helices, which were originally assigned in the CP47/D1/D2 subcomplex (Rhee *et al.* 1998), were in fact the densities of two chlorophylls located towards the N termini of the D1 and D2 proteins. To date this is the only 3D model of a higher plant PS II core complex at a resolution sufficient to reveal its transmembrane helices. However, in 2001 an X-ray structure of PS II isolated from the thermophilic cyanobacterium *Synechococcus elongatus* was published at 3·8 Å resolution (Zouni *et al.* 2001). This work confirmed the positioning of the major subunits within the PS II complex established by cryo-EM, as indicated in Fig. 4, and provided an interpretation of a recent 16 Å projection map derived from 2D crystals of the *S. elongatus* PS II core dimer complex (Da Fonseca *et al.* 2002). It also agreed with the organization of their transmembrane helices deduced by cryo-EM and unambiguously identified the position of the α- and β-subunits of cyt *b*559. As can be seen in Fig. 4, both cryo-EM and X-ray analyses broadly agreed on the positioning of nine other transmembrane helices including a cluster of three at the monomer–monomer interface within the dimer. However, there were some slight differences that may reflect variations between higher plant and cyanobacterial PS II or simply be due to different biochemical isolation procedures. As highlighted in Fig. 4, the cyanobacterial structure has three additional helices close to CP43 compared with that of spinach while an additional helix was found in the peripheral region in the vicinity of helix B of the D1 protein (designated M/N in Fig. 4*a*) in the case of the higher plant system.

Both structures have insufficient resolution to identify amino-acid side-chains and the ordering of the helices of D1/D2/CP43/CP47 in Fig. 4*a* relies on the known ordering of analogous helices in the bacterial and PS I RCs (Deisenhofer *et al.* 1985; Jordan *et al.* 2001). The low resolution of the structural models has not allowed unambiguous assignment of the additional transmembrane helices to specific low-molecular-weight subunits (e.g. PsbH, I, J, K, L, M, N, T_c, W, X and possibly Z) found within the PS II complex (Barber *et al.* 1997; Cinque *et al.* 2001). However, based on other information tentative assignments have been made as shown in Fig. 4 for both the higher plant (Hankamer *et al.* 2001b) and cyanobacterial (Zouni *et al.* 2001) systems.

As shown in Fig. 5*e*, the X-ray analysis was able to reveal density for the PsbV of *S. elongatus* aided by the fact that this extrinsic protein of the oxygen-evolving complex (OEC) is a cytochrome (cyt *c*550) containing a readily detectable haem iron. The extrinsic density in the X-ray map also contained a region of β-strands, making a tube 35 Å long with a diameter of approximately 15 Å tilted at 45° to the membrane plane (see Fig. 5*e*). This feature has tentatively been assigned to approximately half of the PsbO manganese-stabilizing protein, which is known to contain a considerable amount of β-sheet (Bricker & Frankel, 1998; De Las Rivas & Heredia, 1999; Pazos *et al.* 2001).

In the case of higher plants and green algae, information on the structure and organization of the OEC proteins has been derived from cryo-EM using single-particle analyses of the PS II supercomplex isolated from spinach (Nield *et al.* 2001a, 2002). Difference mapping suggests

https://doi.org/10.1017/S0033583502003839 Published online by Cambridge University Press

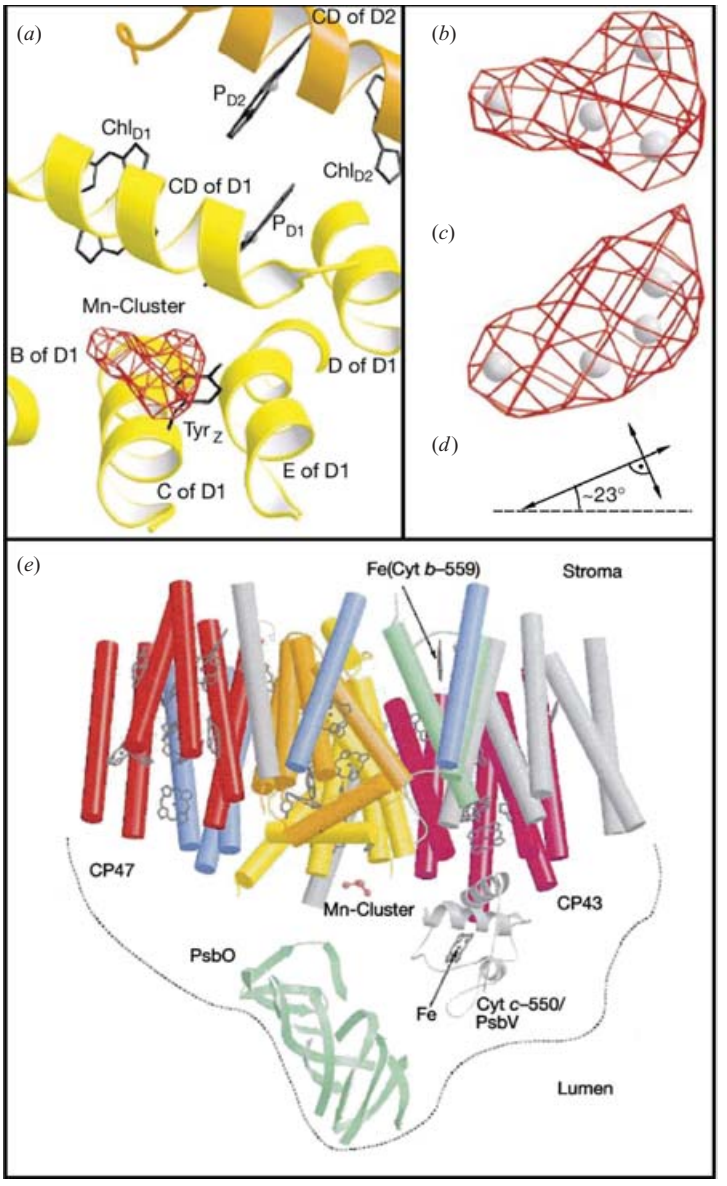

Fig. 5. Location and orientation of the $(Mn)_4$ cluster taken from Zouni *et al.* (2001). (*a*) Close-up view of the reaction centre with the electron density of the $(Mn)_4$ cluster contoured at 5 σ. The view is from the lumenal side onto the membrane plane and shows that the $(Mn)_4$ cluster is located at the lumenal ends of the C and D helices of the D1 protein, close to the surface CD helix as predicted by site-directed mutagenesis (Diner, 2001). (*b*) Enlarged view of the electron density of the manganese cluster. (*c*) 90° rotated around the horizontal axis (view along the membrane with the lumenal side on top). (*d*) Orientation of the short and long axes of (*c*). The latter is tilted 23° against the lumenal side of the membrane plane (hatched line). (*e*) Side view of the PS II monomer looking down the long axis of the D1/D2 proteins with a slightly tilted angle of the membrane plane so as to show the lumenal surface and the positioning of the $(Mn)_4$ cluster, the PsbO protein assigned to the β-sheet structure (green) and cyt *c*550 (PsbV). The cylinders show the transmembrane helices of the various subunits within the monomer and can be compared with the lumenal view shown in Fig. 4*b* (note that the colour coding is slightly different). (The figure is taken from Zouni *et al.* 2001, and modified by labelling.)

https://doi.org/10.1017/S0033583502003839 Published online by Cambridge University Press

that a single copy of the PsbO protein lies along the lumenal surface of the PS II core complex stretching from the CP47 side, across the lumenal loops of the D1/D2 proteins to the region adjacent to CP43. A calculated remote model of the PsbO protein (Pazos *et al.* 2001) has been fitted into the available density and suggests the molecule is elongated with an overall length in the region of 80 Å and a width of approximately 15–20 Å. The remaining extrinsic mass observed in the 3D model derived from single-particle analysis has been attributed to single copies of the PsbP and PsbQ OEC proteins and to the lumenal loops of the intrinsic RC core proteins, particularly the very large loops joining helices 5 and 6 of CP43 and CP47. Although there is some consistency between the positioning of the PsbO protein in the cyanobacterial X-ray and the higher plant cryo-EM models, the latter differs in that there is no evidence to suggest that a portion of the PsbO protein protrudes at an angle of approximately 45° from the membrane surface. One possibility for this difference between the two structures is that the PsbO protein is sufficiently flexible to exist in different conformational states within the PS II complex (Bricker & Frankel, 1998). Moreover, there has been a series of studies reviewed by Bricker & Frankel (1998) that suggest there may be two copies of the PsbO per PS II RC, but to date the EM and X-ray structures do not support this stoichiometry.

5. Organization of chlorophylls and redox active cofactors

The first direct structural information on the organization of the PS II chlorophylls and other cofactors came from electron crystallography studies (Rhee *et al.* 1998). At 8 Å resolution it was possible to observe the densities of the porphyrin head groups of the bound chlorins. Within the D1/D2 helices, six densities were assigned, arranged around the two-fold axis that related the D1 and D2 helices in a manner similar to that observed for cofactors within the purple bacterial RC. Importantly, however, it was noted that there was no 'special pair' and that the four chlorophylls on the electron donor side of the RC were equally spaced at approximately 11 Å centre-to-centre. In the case of the two densities assigned to pheophytin, however, their positioning seemed to match that of their counterparts in the bacterial RC. The CP47 subunit is a chlorophyll-binding protein and 14 densities within the electron density map were suggested to be due to the tetrapyrrole head groups of the bound chlorophylls. These chlorophylls were organized in layers towards the stromal and lumenal surfaces and follow the trend for histidine locations in this protein (Barber *et al.* 2000). The X-ray diffraction analyses (Zouni *et al.* 2001) confirmed and extended these conclusions. Not only did the X-ray data give more accurate information about the positioning and orientations of the four chlorophylls and two pheophytin molecules clustered within the D and E transmembrane helices of the D1 and D2 proteins, it confirmed the existence of two additional chlorophyll molecules, probably ligated to D1–His118 and D2–His117 residues, usually referred to as $Chl_{Z\text{-}D1}$ and $Chl_{Z\text{-}D2}$ (see Fig. 6). Also as indicated in Figs. 5 and 6, the X-ray structure unambiguously located the haem irons of cyt *b*559 and cyt *c*550 (PsbV) as well as the non-haem iron centrally positioned between the Q_A and Q_B binding sites on the D2 and D1 proteins respectively. Densities were tentatively assigned to the Q_A plastoquinone and to D1–Tyr161 (Y_Z) and the two-fold related D2–Tyr160 (Y_D). As in the case of earlier cryo-EM work, 14 chlorophylls were shown to be bound to CP47 and in addition 12 or 13 chlorophylls were identified within the six-helical bundle of CP43.

As mentioned earlier, perhaps the most important outcome of the X-ray diffraction analysis to date was the assignment of a density to the $(Mn)_4$ cluster and that this density was located close to the CD surface helix joining transmembrane helices C and D of the D1 protein (see

https://doi.org/10.1017/S0033583502003839 Published online by Cambridge University Press

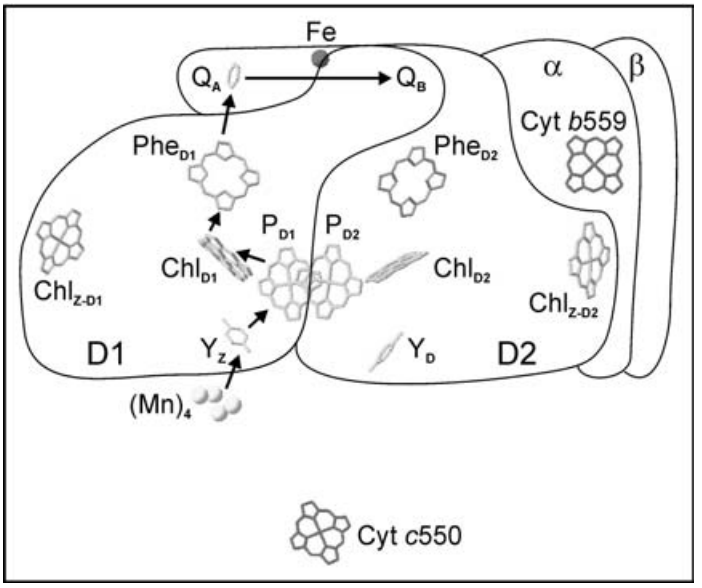

Fig. 6. Organization of the RC cofactors of PS II based on the X-ray model at 3·8 Å resolution (Zouni *et al.* 2001). The arrow shows the direction of electron transfer from the $(Mn)_4$ cluster to the terminal plastoquinone acceptor Q_B. This latter quinone was not present in the 3D crystals analysed but its position is inferred from the similarity in the structures of PS II and the purple bacterial reaction centres (Diesenhofer *et al.* 1985). An outline of the D1-, D2-, α- and β-subunits has been drawn to emphasize each protein–cofactor relationship in a diagrammatic manner.

Fig. 5*a*) as predicted by a wide range of experiments (Diner, 2001). The electron density map also supported earlier predictions that the C terminus of the D1 protein could possibly provide ligands for the $(Mn)_4$ cluster as well as residues in or close to the CD surface helix (Diner, 2001). Confirmation that the density was due to Mn was obtained by measuring X-ray edge anomalous diffraction.

The electron density in the X-ray derived map was shaped such that it can accommodate three Mn atoms at the corners of an isosceles triangle with a fourth placed at the centre of the triangle (see Fig. 5*b*, *c*). This arrangement and the inter-atomic distances are consistent with recent predictions arising from electron paramagnetism, ENDOR and X-ray spectroscopy (Carrell *et al.* 2001; Peloquin & Britt, 2001; Robblee *et al.* 2001). Although, as explained above, Ca^{2+} is known to be an important cofactor in the water oxidase reaction and located close to the $(Mn)_4$ cluster it has not yet been detected in the X-ray structure.

6. Implications arising from the structural models

(1) The main subunits of the PS II RC core are arranged such that the transmembrane helices of the CP47/D2 proteins are related by a pseudo-twofold axis to the transmembrane helices of CP43/D1 proteins. This structural arrangement is similar to that found for the 11 transmembrane helices of the PS I RC proteins PsaA and PsaB[8] indicative of a common evolutionary origin (Rhee *et al.* 1998; Schubert *et al.* 1998).

(2) Although the main cofactors of the PS II RC are arranged around a twofold axis similar to that found in the purple bacterial RC (see Fig. 6), P680 is not a 'special pair' of

https://doi.org/10.1017/S0033583502003839 Published online by Cambridge University Press

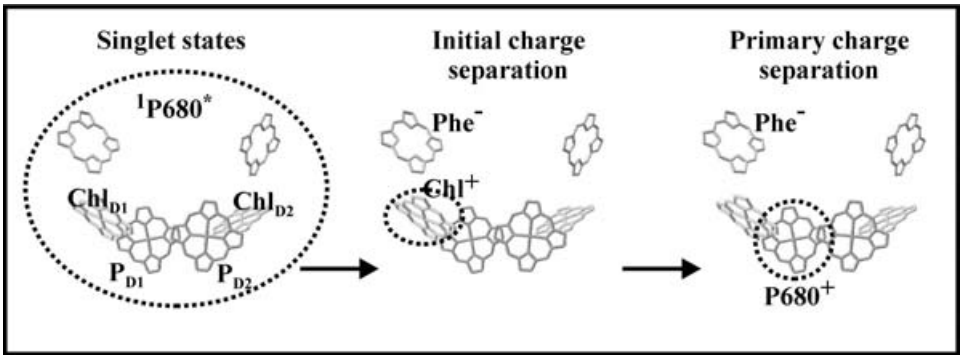

Fig. 7. Scheme for primary charge separation in PS II emphasizing that the initial electron donor to Phe is Chl_{D1} and that the subsequent 'hole' migration generates $P680^{\bullet+}$ mainly localized on the P_1 chlorophyll ligated to D1–His198.

excitonically coupled chlorins as found in the bacterial system or in the RC of PS I. This difference could be due to the requirement of P680 to generate a radical cation having a very high redox potential (Barber & Archer, 2001; Barber, 2002).

(3) The absence of a 'special pair' results in a shallow trap such that PS II has a relatively high chlorophyll fluorescence yield compared with other types of photosystem. Delocalization of the excited state of P680 (P680*) (Durrant *et al.* 1995; Dekker & Van Grondelle, 2000) suggests that initial charge separation could occur from the accessory chlorophyll (Chl_{D1}) (see Fig. 7) for which there is recent experimental evidence (Prokhorenko & Holzwarth, 2000; Diner *et al.* 2001). The radical cation may then induce oxidation of P_{D1} or P_{D2} chlorophylls before electron abstraction from Y_Z or Y_D. If true, this series of events makes PS II novel in terms of its primary electron transfer process as compared with other types of photosystems. It also means that all four chlorophylls (Chl_{D1}, Chl_{D2}, P_{D1}, P_{D2}) are high potential species (as discussed by Barber & Archer, 2001).

(4) There is only one $(Mn)_4$ cluster and it is close to D1–Tyr161(Y_Z). However, the distance of 7 Å between the two redox centres is relatively long to accommodate a sequential e/H^+ abstraction from water bound to the $(Mn)_4$ cluster, as discussed above. Clearly higher resolution structures are required to identify the ligands and protein environment of the $(Mn)_4$ cluster in order to develop improved postulates for the water-oxidation process and related e/H^+ transfer reactions.

(5) When the extrinsic proteins are present, the $(Mn)_4$ cluster is buried within a protein matrix by approximately 30–40 Å from the lumenal surface (Zouni *et al.* 2001; Nield *et al.* 2002). However, the precise role of this protein shield is not yet fully understood although it is well established that the OEC proteins facilitate the availability of Ca^{2+} and Cl^- as co-factors for the water-oxidation reaction.

(6) Although positioned some way from the P680 chlorophylls (see Fig. 3) $Chl_{Z\text{-}D1/D2}$ (approximately 25 Å) and cyt *b*559 (approximately 40 Å) can be photo-oxidized with ms kinetics under some conditions (Telfer *et al.* 1991; Hanley *et al.* 1999; Tracewell *et al.* 2001). According to electron transfer theory (Moser *et al.* 1992) for these oxidations to occur in the ms time domain, intermediate electron carriers are needed. Over the past couple of years this has stimulated a number of experiments with the current view being that β-carotene molecules known to be bound to the D1/D2 protein, but not reported in the published 3·8 Å X-ray derived model of Zouni *et al.* (2001), act as intermediate electron

https://doi.org/10.1017/S0033583502003839 Published online by Cambridge University Press

transport carriers. Whether electrons go from cyt *b*559 to P680 via $Chl_{Z\text{-}D2}$ or directly via β-carotene is a matter of intense debate at present.

(7) Cyt *c*550 (PsbV) is also positioned a lengthy distance from P680 (approximately 28 Å) although in this case there is no report of this cytochrome undergoing PS II-driven photo-oxidation. Therefore its function remains an enigma.

(8) The high-resolution structural models are aiding the interpretation of 3D structures of larger PS II complexes that consist of the core dimer and light-harvesting proteins. In particular, a light-harvesting complex II (LHC II)–PS II supercomplex has been isolated from higher plants and green algae which has been studied by EM and single-particle analysis (Nield *et al.* 2000a, b, 2002). Figure 8 shows a 3D structure of the LHC II–PS II supercomplexes isolated from spinach. It has a molecular mass of approximately 1000 kDa, contains a centrally located PS II core dimer and in each flanking region the chl *a*/*b* binding (Cab) proteins LHC II, CP26 and CP29 (Hankamer *et al.* 1997a, b). The precise positioning of these Cab proteins is unknown but the electron density within the 17 Å structure is consistent with one LHC II trimer and a monomer of CP29 and CP26, as indicated in Fig. 8. This supercomplex contains approximately 100 chlorophylls per PS II RC of which approximately 75 are chl *a* and 25 chl *b*. Interestingly the low-molecular-weight transmembrane helical protein detected in the spinach core (highlighted and designated M/N in Fig. 4*a*), but not in the cyanobacterial structure, seems to make a link between the flanking Cab proteins and the PS II RC core. If this small subunit binds chlorophyll as do many of the low-molecular-weight subunits of PS I (Jordan *et al.* 2001), then perhaps it functions as an 'excitonic bridge' to facilitate energy transfer to the RC. Since cyanobacteria do not contain Cab proteins but have extrinsic phycobiliproteins as an outer light-harvesting system then this small subunit, detected in spinach PS II, would not be required. Perhaps the additional three low-molecular-weight subunits of *S. elongatus* not found in spinach PS II (highlighted in Fig. 4*b*) play a role in structurally and functionally linking the phycobilisomes to the PS II core dimer. In any event, work on the LHC II–PS II supercomplex and related studies on even larger PS II complexes and arrays (Boekema *et al.* 2000; Yakushevska *et al.* 2001) is helping to build a structural model to show how the LHC II–PS II supercomplex and additional LHC II trimers come together to form a complete PS II unit within natural photosynthetic membranes of higher plants.

7. Perspectives

In many respects the recently published X-ray structure has not revealed any significant surprises since previous spectroscopic and molecular biological analyses, together with the cryo-EM work and analogy of the purple bacterial RC have provided a reasonably accurate structural model of PS II (Barber & Kühlbrandt, 1999). The challenge now is to obtain a higher resolution X-ray structure which will reveal amino-acid side-chains and thus allow a detailed understanding of how the various cofactors and chlorophyll molecules within PS II relate with their protein environment. This information is needed particularly for the $(Mn)_4$ cluster where the ultimate goal will be to identify the substrate water molecules before and during their oxidation so that the molecular basis of the S-state transitions will be understood. I have no doubt this information will be available soon.

In addition to the above challenge there are other facets of PS II function which will also require a structural understanding. The rapid turnover of the D1 protein is truly a remarkable

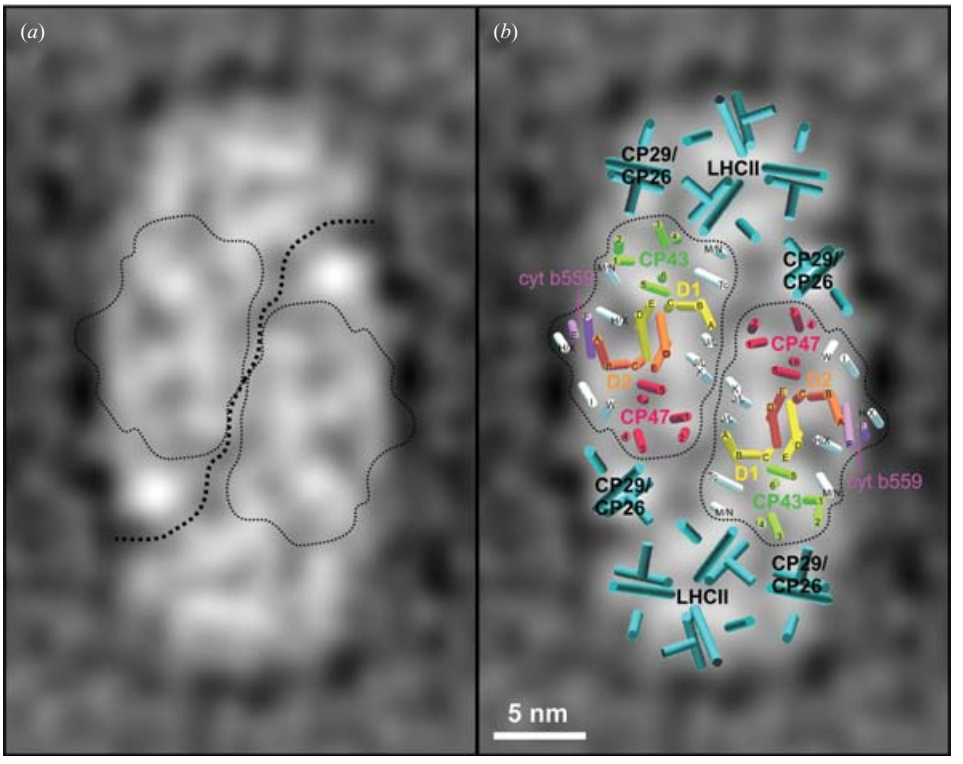

Fig. 8. The relationship between the transmembrane helices of the central PS II core dimer and those of the outer antenna system of the LHC II–PS II supercomplex of spinach based on a combination of electron crystallographic and single particle analyses. (*a*) 2D top view projection derived from a 17 Å 3D map of the LHC II–PS II supercomplex obtained by cryo-EM showing the transmembrane domain (Nield *et al.* 2000c). The large dotted line separates the two monomers that make up the supercomplex and the fine dotted lines outline the central position of the core dimer. (*b*) Helices of the spinach core dimer from Fig. 4*a* and the antenna Cab proteins, Lhcb1, 2, 4 and 5, based on the structure of LHC II (Kühlbrandt *et al.* 1994), incorporated into the projection shown in (*a*) along the lines of previous modelling, but with modifications (Nield *et al.* 2000a, b; Hankamer *et al.* 2001a, b). For the helices of the core dimer, the colour coding and labelling is the same as in Fig. 4*a*, while the modelled helices for LHC II, CP29 and CP26 (including one surface helix) are in cyan. Of special note is that according to the modelling, a group of two low-molecular-weight subunits (tentatively labelled T_C and M/N) adjacent to helix B of the D1 protein seems to form a structural link to the LHC II trimer. In contrast, *S. elongatus* has only one transmembrane helix assigned to this region (see Fig. 4*b*).

dynamic property of PS II resulting from the toxic nature of the water-oxidizing reaction (Barber & Andersson, 1992; Barber, 1994; Andersson & Barber, 1996). As yet the cryo-EM and X-ray structures do not help us to understand this unique property other than the conclusion that CP43 lays adjacent to the D1 protein which is believed to be displaced from the complex when D1 protein degradation and replacement occurs (Barbato *et al.* 1992; Zhang & Aro, 2002). The bigger picture is also important since the isolated PS II core complexes used to obtain the high-resolution information normally have light-harvesting antennae systems associated with them when in the intact thylakoid membrane. In the case of *S. elongatus* the light-harvesting system is composed of C-allophycocyanin and C-phycocyanin which together make up its phycobilisome. As diagrammatically shown in Fig. 1*b*, the size of the phycobilisome relative to the PS II core complex is massive and is known to bind to the surface of the dimeric

https://doi.org/10.1017/S0033583502003839 Published online by Cambridge University Press

form of the core. How and where the phycobilisome attaches and interacts with the stromal surface of the core dimer in this, and other cyanobacteria and red algae, has yet to be determined. In the case of higher plants and green algae our understanding of the macromolecular structure is much better. The structures of supermolecular complexes containing Cab proteins have been investigated using EM and reasonable models have been achieved, aided by the incorporation of high-resolution structural data of their components (Nield *et al.* 2000a–c, 2001; Boekema *et al.* 2000; Yakushevska *et al.* 2001). In all systems studied the PS II core complex seems to function *in vivo* as a dimer, but the significance of this dimerization has yet to be revealed.

8. Acknowledgements

I thank the Biotechnology and Biological Research Council (BBSRC) for financial support. I also acknowledge and thank my colleagues who have worked with me on the structure of higher plant PS II, particularly Ben Hankamer, Jon Nield, Ed Morris, Paula da Fonseca, Claudia Büchel, Kyong-He Rhee and Werner Kühlbrandt. I also thank Jon Nield for assisting in the production of the figures.

9. Addendum

Since completing the review Kamiya & Shen (In Press), have reported a new 3·7 Å structural model of PS II determined by X-ray crystallography. The dimeric PS II core complex used was isolated from the thermophilic cyanobacterium *Synechococcus vulcanus* (now renamed *Thermosynechococcus vulcanus*). The new structure is in general agreement with the X-ray model for *S. elongatus* determined by Zouni *et al.* (2001). However more density has been traced and assigned, particularly for the extrinsic domain on the lumenal surface. The 33 kDa PsbO protein has been confirmed to consist of a large amount of β-strand but a short helix was found towards the C-terminus. Using polyalanine, 83·3% of the total residues of the PsbO protein have been modelled resulting in a cylindrical structure with dimensions of 20 Å diameter and 45 Å length with a 25 Å loop extending from one side of the cylinder. This new work has also revealed for the first time the positioning and structure of the 12 kDa extrinsic PsbU protein. It was found to have an all α architecture composed of five or more short α-helices. This protein links the PsbO and cyt *c*550 (PsbV) proteins and is 30 Å from the lumenal surface. Together with the lumenal regions of CP47, CP43, D1 and D2 proteins, the three extrinsic subunits shield the Mn cluster from the bulk solution. This work emphasizes again that there is only a single copy of each of these extrinsic proteins in the PS II complex.

The density assigned to the Mn cluster is similar in shape to that reported by Zouni *et al.* (2001) supporting the suggestion that three Mn atoms are positioned in the corner of the density and one in the centre. However Kamiya & Shen (In Press) find all four postulated Mn atoms to be coplanar while the structural model of Zouni *et al.* (2001) suggest that the central Mn protrudes towards the lumenal surface of the membrane. Kamiya and Shen also conclude that the Mn cluster may be exclusively co-ordinated by the D1 protein and propose 4 or 5 amino-acid residues that provide the ligands; D1–Ala344, D1–Asp170, D1–Glu333 (or His332) and possibly D1–His337, D1–Asp189 (or His190). They note that Tyr73 located in the loop joining the lumenal ends of transmembrane helices A and B of the D1 protein is also positioned close to the Mn cluster. The idea that the C-terminal residue of the D1 protein provides ligands

for the Mn cluster is consistent with the inability of mutants unable to process the C-terminus of the D1 protein to assemble the Mn cluster (Metz & Seibert, 1984) and with the effects of site-directed mutations in this region (Diner, 2001). In fact the finding that the C-terminal residue of the D1 protein Ala344 becomes available as a ligand after processing provides a mechanism by which PS II can regulate the assembly of the Mn cluster during the turnover of the D1 protein. The C-terminal processing exposing Arg344 occurs after the newly synthesized D1 protein is inserted into the previously photodamaged PS II (Matoo & Edelman, 1987) and presumably in this way initiates assembly of the Mn cluster.

The new structure confirms the positioning of the main cofactors bound within the PS II proteins as described by Zouni *et al.* (2001) but in addition revealed an extra chlorophyll in CP47 giving a total of 16. Both analyses assign 13 chlorophylls bound to CP43. However, of considerable importance has been the assignment of density of two β-carotene molecules; one modelled as a *cis*- and one as an all-*trans* isomer. Surprisingly these two β-carotenes are located close to each other with a minimum distance of 5 Å. In recent years, a dogma emerged which implied the β-carotenes in the PS II reaction centre were located such that one was associated with the D1 protein and one with the D2 protein, possibly related by a pseudo-twofold axis which relates the D1 and D2 subunits (Telfer, 2002). The new X-ray map does not support this dogma and places the two β-carotenes on the D2 side. In this way they are strategically placed to facilitate electron flow from either cyt *b*559 or $Chl_{Z\text{-}D2}$ to the primary oxidant. The estimated distances favour electron flow from cyt *b*559 and $Chl_{Z\text{-}D2}$ directly to P680 via the β-carotene rather than a branched pathway (Faller *et al.* 2001; Tracewell *et al.* 2001). From this structural information it can be concluded that the oxidation of $Chl_{Z\text{-}D1}$ is unlikely to occur as had previously been thought (Stewart *et al.* 1998).

10. References

Andersson, B. & Barber, J. (1996). Mechanisms of photodamage of protein degradation during photoinhibition of photosystem two. In: *Advances in Photosynthesis Series: Photosynthesis and the Environment* (ed. N. R. Baker), pp. 101–121. Dordrecht: Kluwer.

Barbato, R., Friso, G., Rigoni, F., Dalla Vecchia, F. & Giacometti, G. M. (1992). Structural changes and lateral redistribution of PSII during donor side photoinhibition of thylakoids. *J. Cell Biol.* **119**, 325–335.

Barber, J. (2002). P680: What is it and where is it? *Bioelectrochem.* **55**, 135–138.

Barber, J. (1987). Photosynthetic reaction centres: a common link. *Trends biochem. Sci.* **12**, 321–326.

Barber, J. (1994). Molecular basis of the vulnerability of photosystem II to damage by light. *Aust. J. Plant Physiol.* **22**, 201–208.

Barber, J. & Andersson, B. (1992). Too much of a good thing: light can be bad for photosynthesis. *Trends biochem. Sci.* **17**, 61–66.

Barber, J. & Archer, M. D. (2001). P680, the primary electron donor of photosystem II. *J. photochem. Photobiol. (A)* **142**, 97–106.

Barber, J. & De Las Rivas, J. (1993). A functional model for the role of cyt b559 in the protection against donor and acceptor side photoinhibition. *Proc. natn. Acad. Sci. USA* **90**, 10942–10946.

Barber, J. & Kühlbrandt, W. (1999). Photosystem II. *Curr. Opin. struct. Biol.* **9**, 469–475.

Barber, J., Morris, E. P. & Büchel, C. (2000). Revealing the structure of the photosystem two chlorophyll binding proteins, CP43 and CP47. *Biochim. Biophys. Acta* **1459**, 239–247.

Barber, J., Nield, J., Morris, E. P., Zheleva, D. & Hankamer, B. (1997). The structure, function and dynamics of photosystem II. *Physiol. Pl.* **100**, 817–827.

Boekema, E. J., Van Breemen, J. F. L., Van Roon, H. & Dekker, J. P. (2000). Arrangement of PSII in crystalline macrodomains within the thylakoid membrane of green plant chloroplasts. *J. molec. Biol.* **301**, 1123–1133.

Bricker, T. M. & Frankel, L. K. (1998). The structure and function of the 33 kDa extrinsic protein of photosystem II: a critical assessment. *Photosyn. Res.* **56**, 157–173.

Carrell, T. G., Tyryshkin, A. M. & Dismukes, G. C. (2001). An evolution of structural models for the photosynthetic water-oxidising complex derived from spectroscopic X-ray diffraction signatures. *J. biol. inorg. Chem.* **7**, 2–22.

https://doi.org/10.1017/S0033583502003839 Published online by Cambridge University Press

Cinque, G., Muller, B., Eichacker, L. A., Stern, D. B., Bassi, R., Herrmann, R. G. & Wollman, F. A. (2001). The chloroplast gene ycf9 encodes a PSII core subunit, PsbZ, that participates in PSII supramolecular architecture. *Plant Cell* **13**, 1347–1367.

Da Fonseca, P., Morris, E. P., Hankamer, B. & Barber, J. (2002). Electron crystallographic study of photosystem II of the cyanobacterium *Synechococcus elongatus*. *Biochemistry* **41**, 5163–5167.

Debus, R. J. (1992). The manganese and calcium ions of photosynthetic oxygen evolution. *Biochim. Biophys. Acta* **1102**, 269–352.

Deisenhofer, J., Epp, O., Miki, K., Huber, R. & Michel, H. (1985). Structure of the protein subunits in the photosynthetic reaction centre *Rhodopseudomonas viridis* at 3 Å resolution. *Nature* **318**, 618–624.

Dekker, J. P. & Van Grondelle, R. (2000). Primary charge separation in photosystem II. *Photosyn. Res.* **63**, 195–208.

De Las Rivas, J. & Heredia, P. (1999). Structural predictions on the 33 kDa extrinsic protein associated with the oxygen evolving complex of photosynthetic organisms. *Photosyn. Res.* **61**, 11–21.

Diner, B. A. (2001). Amino acid residues involved in the coordination and assembly of the manganese cluster of photosystem II. Proton-coupled electron transport of the redox-active tyrosines and its relationship to water oxidation. *Biochim. Biophys. Acta* **1503**, 147–163.

Diner, B. A. & Babcock, G. T. (1996). Structure, dynamics and energy conversion efficiency in photosystem II. In: *Advances in Photosynthesis, Vol. 4: The Light Reactions 1996* (eds. D. R. Ort & C. F. Yocum), pp. 213–247. Dordrecht: Kluwer Academic.

Diner, B. A., Schlodder, E., Nixon, P. J., Coleman, W. J., Rappaport, F., Lavergne, J., Vermaas, W. F. J. & Chisholm, D. A. (2001). Site-directed mutations at D1-His189 and D2His197 of photosystem II in *Synechocystis* PCC 6803: sites of primary charge separation and cation and triplet stabilization. *Biochemistry* **40**, 9265–9281.

Durrant, J. R., Klug, D. R., Kwa, S. L. S., Van Grondelle, R., Porter, G. & Dekker, J. P. (1995). A multimer model for 680, the primary electron donor of photosystem II. *Proc. natn. Acad. Sci. USA* **92**, 4798–4802.

Faller, P., Pascal, A. & Rutherford, A. W. (2001). β-carotene redox reactions in photosystem II: electron transfer pathway. *Biochemistry* **40**, 6431–6440.

Hankamer, B., Barber, J. & Boekema, E. J. (1997b). Structure and membrane organisation of PSII in green plants. *Annu. Rev. Plant Physiol. molec. Biol.* **48**, 641–671.

Hankamer, B., Morris, E. P. & Barber, J. (1999). Cryo-electron microscopy of photosystem two shows that CP43 and CP47 are located on opposite sides of the D1/D2 reaction centre proteins. *Nature struct. Biol.* **6**, 560–564.

Hankamer, B., Morris, E. P., Nield, J., Carne, A. & Barber, J. (2001b). Subunit positioning and transmembrane helix organisation in the core dimer of Photosystem II. *FEBS Lett.* **504**, 142–151.

Hankamer, B., Morris, E. P., Nield, J., Gerle, C. & Barber, J. (2001a). Three-dimensional structure of photosystem II core dimer of higher plants determined by electron microscopy. *J. struct. Biol.* **135**, 262–269.

Hankamer, B., Nield, J., Zheleva, D., Boekema, E. J., Jansson, S. & Barber, J. (1997a). Isolation and biochemical characterisation of monomeric and dimeric PSII complex from spinach and their relevance to the organisation of photosystem II in vivo. *Eur. J. Biochem.* **243**, 422–429.

Hanley, J., Deligiannakis, Y., Pascal, A., Faller, P. & Rutherford, A. W. (1999). Carotenoid oxidation in photosystem II. *Biochemistry* **38**, 8189–8195.

Hanmann, M. & Junge, W. (1999). Photosynthetic water oxidation: a simplex-scheme of its partial reactions. *Biochim. Biophys. Acta* **1411**, 86–91.

Hoganson, C. W. & Babcock, G. T. (1997). A metalloradical mechanism for the generation of oxygen from water in photosynthesis. *Science* **277**, 199–219.

Hu, Q., Miyashita, H., Iwasaki, I., Kurano, N., Miyachi, S., Iwaki, M. & Itoh, S. (1998). A photosystem I reaction center driven by chlorophyll d in oxygenic photosynthesis. *Proc. natn. Acad. Sci. USA* **95**, 13319–13323.

Jordan, P., Fromme, P., Witt, H.-T., Klukas, O., Saenger, W. & Kraus, N. (2001). Three-dimensional structure of cyanobacterial photosystem I at 2·5 Å resolution. *Nature* **411**, 909–916.

Kamiya, N. & Shen, J.-R. (In Press). Crystal structure of oxygen-evolving photosystem II from *Thermosynechococcus vulcanus* at 3·7 Å resolution. *Proc. natn. Acad. Sci. USA*.

Kapazoglou, A., Sagloico, F. & Dure, L. (1995). PSII-T, a new nuclear encoded lumenal protein from PSII. *J. biol. Chem.* **270**, 12197–12201.

Kok, B., Forbush, B. & McGloin, M. (1970) Cooperation of charges in photosynthetic oxygen evolution. A linear four step mechanism. *Photochem. Photobiol.* **11**, 457–475.

Krauss, N., Schubert, W.-D., Klukas, O., Fromme, P., Witt, H. T. & Saenger, W. (1996). Photosystem I at 4 Å resolution represents the first structural model of a joint photosynthetic reaction centre and core antenna system. *Nature struct. Biol.* **3**, 965–973.

Kühlbrandt, W., Wang, D. N. & Fujiyoshi, Y. (1994). Atomic model of plant light harvesting complex by electron crystallography. *Nature* **367**, 614–621.

Ljungberg, U., Akerlund, H.-E. & Andersson, B. (1986). Isolation and characterisation of the 10 kDa and 22 kDa polypeptides of higher plant photosystem 2. *Eur. J. Biochem.* **158**, 477–482.

Matoo, A. K. & Edelman, M. (1987). Intramembrane translocation and post-translational palmitoylation of

the chloroplast 3 kDa herbicide binding protein. *Proc. natn. Acad. Sci. USA* **84**, 1497–1501.

Metz, J. G. & Seibert, M. (1984). Presence in photosystem II core complexes of a 34 kDa polypeptide required for water photolysis. *Plant Phys.* **76**, 829–832.

Michel, H. & Deisenhofer, J. (1988). Relevance of the photosynthetic reaction center from purple bacteria to the structure of photosystem II. *Biochemistry* **27**, 1–7.

Miyashita, H., Ikemoto, H., Kurano, N., Adachi, K., Chihara, M. & Miyachi, S. (1996). Chlorophyll as a major pigment. *Nature* **383**, 402.

Morris, E. P., Hankamer, B., Zheleva, D., Friso, G. & Barber, J. (1997). The 3D structure of a photosystem II core complex determined by electron crystallography. *Structure* **5**, 837–849.

Moser, C. C., Keske, J. M., Warncke, K., Farid, R. S. & Dutton, P. L. (1992). Nature of biological electron transfer. *Nature* **355**, 796–802.

Nield, J., Balsera, M., De Las Rivas, J. & Barber, J. (2002). 3D cryo-EM study of the extrinsic domains of the oxygen-evolving complex of spinach. Assignment of the PsbO protein. *J. biol. Chem.* **277**, 15006–15012.

Nield, J., Kruse, O., Ruprecht, J., Da Fonseca, P., Büchel, C. & Barber, J. (2000b). 3D structure of *Chlamydomonas reinhardtii* and *Synechococcus elongatus* photosystem II complexes allow for comparison of their OEC organisation. *J. biol. Chem.* **275**, 27940–27946.

Nield, J., Orlova, E., Morris, E. P., Gowen, B., Van Heel, M. & Barber, J. (2000a). 3D map of the plant photosystem two supercomplex obtained by cryo-electron microscopy and single particle analyses. *Nature struct. Biol.* **7**, 44–47.

Nield, J. N., Funk, C. & Barber, J. (2000c). Supermolecular structure of photosystem II and location of the PsbS protein. *Phil. Trans. Roy. Soc. London* **355**, 1337–1344.

Pazos, F., Heredia, P., Valencia, A. & De Las Rivas, J. (2001). Threading structural model of the Mn-stabilising protein PsbO reveals presence of two possible beta-sandwich domains. *Proteins: Struct., Funct. Genet.* **45**, 372–381.

Peloquin, J. M. & Britt, R. D. (2001). EPR/ENDOR characterisation of the physical and electronic structure of the OEC $(Mn)_4$-cluster. *Biochim. Biophys. Acta* **1503**, 96–111.

Prokhorenko, V. I. & Holzwarth, A. R. (2000). Primary processes and structure of photosystem II reaction center: a photon echo study. *J. phys. Chem.* (*B*) **104**, 11563–11578.

Rhee, K.-H. (2001). Photosystem II: The solid structural era. *Annu. Rev. biomolec. Struct.* **30**, 307–328.

Rhee, K.-H., Morris, E. P., Barber, J. & Kühlbrandt, W. (1998). Three dimensional structure of the photosystem II reaction centre at 8 Å. *Nature* **396**, 283–286.

Rhee, K.-H., Morris, E. P., Zheleva, D., Hankamer, B., Kühlbrandt, W. & Barber J. (1997). Two dimensional structure of plant photosystem II at 8 Å resolution. *Nature* **389**, 522–526.

Robblee, J. H., Cince, R. M. & Yachandra, V. K. (2001). X-ray spectroscopy-based structure of the $(Mn)_4$-cluster and mechanism of photosynthetic oxygen evolution. *Biochim. Biophys. Acta* **1503**, 7–23.

Saenger, W., Jordan, P. & Krauss, N. (2002). The assembly of protein subunits and cofactors in photosystem I. *Curr. Opin. struct. Biol.* **12**, 244–254.

Schubert, W.-D., Klukas, O., Saenger, W., Witt, H. T., Fromme, P. & Krauss, N. (1998). A common ancestor for oxygenic and anoxygenic photosynthetic systems – a comparison based on the structural model of photosystem I. *J. molec. Biol.* **280**, 297–314.

Stewart, D. H. & Brudvig, G. W. (1998). Cytochrome *b559* of photosystem II. *Biochim. Biophys. Acta* **1367**, 63–87.

Stewart, D. H., Cua, A., Chisholm, D. A., Diner, B. A., Bocian, D. F. & Brudvig, G. W. (1998). Identification of histidine 118 in the D1 polypeptide of photosystem II as the axial ligand to chlorophyll Z. *Biochemistry* **37**, 10040–10046.

Telfer, A. (2002). What is β-carotene doing in photosystem two reaction centres? *Phil. Trans. R. Soc. London* (*B*) **357**, 1431–1440.

Telfer, A., De Las Rivas, J. & Barber, J. (1991). Beta-carotene within the isolated photosystem II reaction centre: photooxidation and irreversible bleaching of this chromophore by oxidised P680. *Biochim. Biophys. Acta* **1060**, 106–114.

Tommos, C. & Babcock, G. T. (2000). Proton and hydrogen currents in photosynthetic water oxidation. *Biochim. Biophys. Acta* **1458**, 199–219.

Tracewell, C. A., Cua, A., Stewart, D. H., Docian, D. F. & Brudvig, G. W. (2001). Characterisation of carotenoid and chlorophyll photooxidation in photosystem II. *Biochemistry* **40**, 193–203.

Vrettos, J. S., Limburg, J. & Brudvig, G. W. (2001). Mechanism of photosynthetic water oxidation: combining biophysical studies of photosystem II with inorganic model chemistry. *Biochim. Biophys. Acta* **1503**, 229–245.

Yakushevska, A. E., Hensen, P. E., Keegstra, W., Van Roon, H., Scheller, H. V., Boekema, E. J. & Dekker, J. P. (2001). Supermolecular organisation of PS II and its associated light-harvesting antenna in *Arabidopsis thaliana*. *Eur. J. biochem.* **268**, 6020–6028.

Zhang, L. & Aro, E.-M. (2002). Synthesis, membrane insertion and assembly of the chloroplast-encoded D1 protein into photosystem II. *FEBS Lett.* **512**, 13–18.

Zouni, A., Witt, H.-T., Kern, J., Fromme, P., Krauss, N., Saenger, W. & Orth, P. (2001). Crystal structure of photosystem II from *Synechococcus elongatus* at 3·8 Å resolution. *Nature* **409**, 739–742.

https://doi.org/10.1017/S0033583502003839 Published online by Cambridge University Press